

Supporting Information

Dually Crosslinked Self-Healing Hydrogels Originated from Cell-Enhanced Effect

*Chen Xu,^{‡b} Qing Li,^{‡a} Xin-Ting Hu,^b Cai-Feng Wang^a and Su Chen^{*a}*

^a State Key Laboratory of Materials-Oriented Chemical Engineering, College of Chemistry and Chemical Engineering, Nanjing Tech University, Nanjing 210009, People's Republic of China

^b State Key Laboratory of Pharmaceutical Biotechnology and School of Life Sciences, Nanjing University, Nanjing 210023, People's Republic of China

[‡] These authors contributed equally to the work.

Supporting Figures

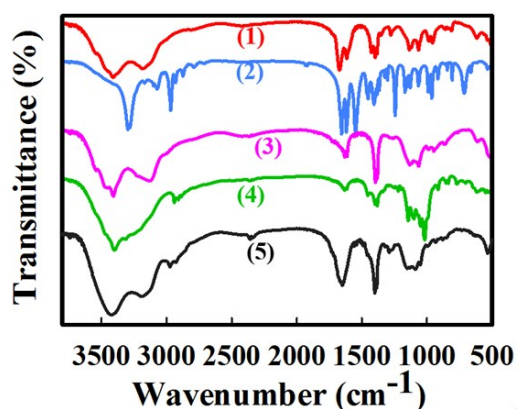


Figure S1. FTIR spectra of (1) AM, (2) NIPAM, (3) NVP, (4) *O*-CMC and (5) *O*-CMC-g-poly(NIPAM-*co*-AM-*co*-NVP) hydrogel.

The FT-IR spectrum of AM presents characteristic absorption peaks at 3195 cm^{-1} reflecting the asymmetric and symmetrical stretch vibration of $-\text{NH}_2$ group, at 1670 cm^{-1} assigned to the stretching vibration of $\text{C}=\text{O}$ group, and at 1430 and 1350 cm^{-1} corresponding to $=\text{C}-\text{H}$ vibration, as indicated in Figure S1 (1). Figure S1 (2) shows the FT-IR spectrum of NIPAM. Characteristic absorption peaks at 2973 and 2935 cm^{-1} corresponding to $-\text{CH}_3$ and $-\text{CH}_2$ vibration, at 1651 cm^{-1} reflecting the asymmetric and symmetrical stretch vibration of $-\text{NH}_2$ group, at 1670 cm^{-1} assigned to the stretching vibration of $\text{C}=\text{O}$ group, and at 1454 cm^{-1} reflecting the stretch vibration of $-\text{CH}-\text{CO}$ group. Figure S1 (3) describes the FT-IR spectrum of NVP. Characteristic absorption bands at 1628 cm^{-1} assigned to the $\text{C}=\text{C}$ absorption, and at 1044 cm^{-1} related to $\text{C}-\text{C}$ peaks on the NVP cyclic structure. The *O*-CMC shows characteristic peaks at 3454 cm^{-1} associated with stretching vibration of $-\text{NH}_2$ and $-\text{OH}$ groups, at 1620 cm^{-1} due to the in-plane bending vibration of $\text{N}-\text{H}$ group and the stretching vibration of $-\text{COOH}$ group, and at 1100 cm^{-1} belonging to the $-\text{C}-\text{O}-$ or bridge- O stretch vibration, as shown in Figure S1 (4). The existence of characteristic bands proves the formation of the expected *O*-CMC-g-poly(NIPAM-*co*-AM-*co*-NVP) hydrogels, as indicated in Figure S1 (5).

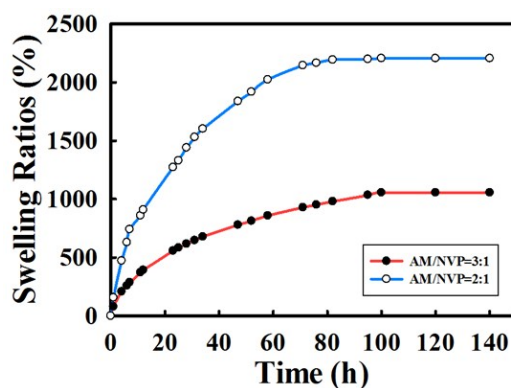


Figure S2. Swelling property of hydrogels.

As shown in Figure S2, the swelling ratios (SRs) of all the samples increase with swelling time. At the initial 30 h of swelling time, the SRs of all the samples increase

sharply. The swelling equilibrium is achieved after 100 h, and the equilibrium SRs for hydrogels with AM/NVP=2:1, 3:1 w/w, are 2213 and 1106%, respectively. The results demonstrate that SRs of *O*-CMC-*g*-poly(NIPAM-*co*-AM-*co*-NVP) hydrogels containing high NVP concentration are larger than those with low NVP concentration.

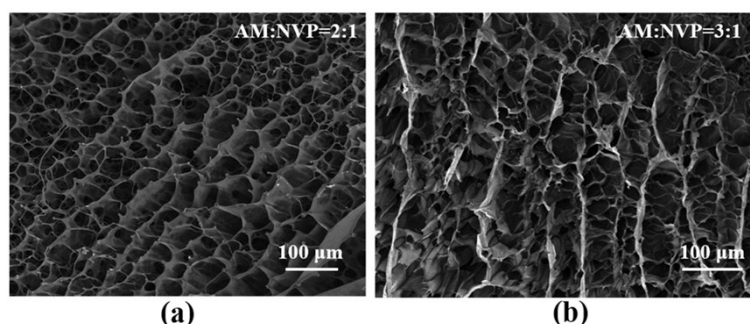


Figure S3. SEM images of hydrogels at different AM/NVP ratios of (a) 2:1 and (b) 3:1 (w/w).

The morphology of *O*-CMC-*g*-poly(NIPAM-*co*-AM-*co*-NVP) hydrogel networks with different AM/NVP weight ratios was investigated by SEM. As shown in Figure S3, the hydrogels at AM/NVP=2:1 and 3:1 w/w present uniform network structures with the pore diameters around 50 and 30 μ m, respectively. The results reveal that the pore diameter decreases as the NVP content decreases. The hydrogels with larger pore diameter exhibit higher degrees of water swelling capability, which is consistent with the swelling ratio results described above.

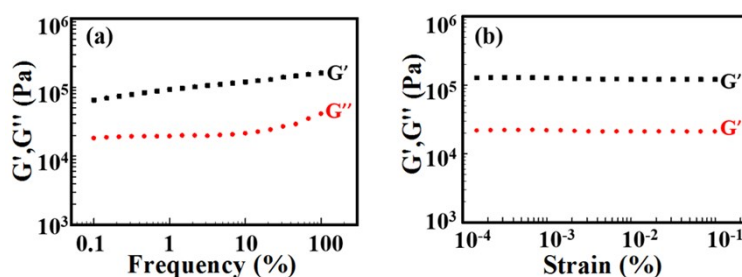


Figure S4. The rheological behavior of hydrogels at AM/NVP = 2:1 (w/w).

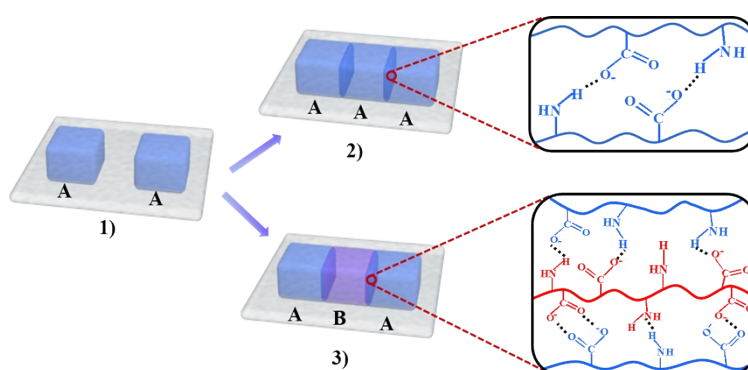


Figure S5. Schematic illustrating the construction of cell-loaded D-hydrogels via hydrogen-bonding interactions between polymer chains and cell secretions, where A means polymer chains and B means cell secretions.

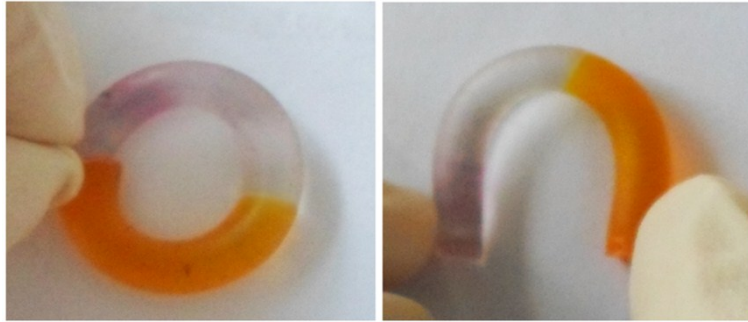


Figure S6. Images demonstrating the self-healing behavior of cell-loaded D-hydrogels with different shapes obtained by bringing the freshly fractured surfaces with different colors into contact.

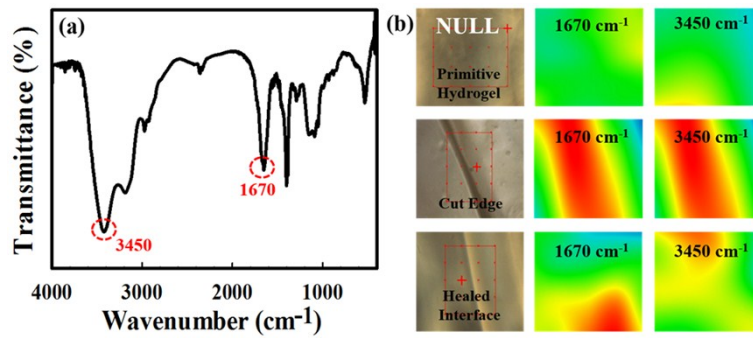


Figure S7. IR spectra, Optical images and IR images of the S-hydrogels before and after self-healing.

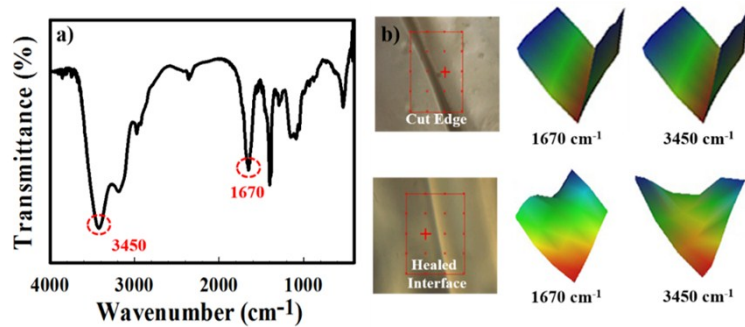


Figure S8. IR spectra, Optical images and 3D IR images of the S-hydrogels before and after self-healing.

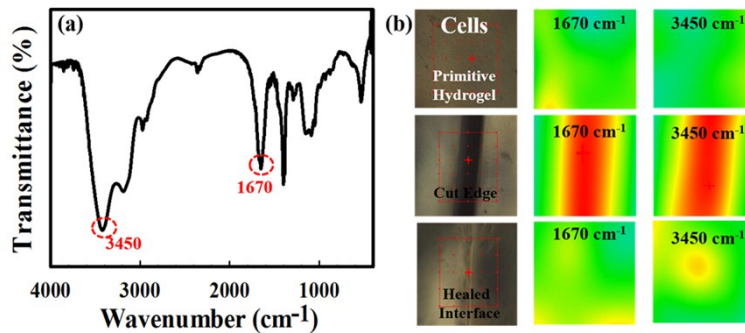


Figure S9. IR spectra, Optical images and IR images of cell-loaded D-hydrogels before and after self-healing.

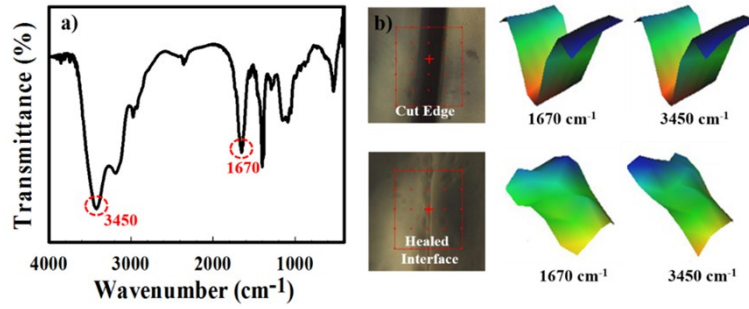


Figure S10. IR spectra, Optical images and 3D IR images of cell-loaded D-hydrogels before and after self-healing.

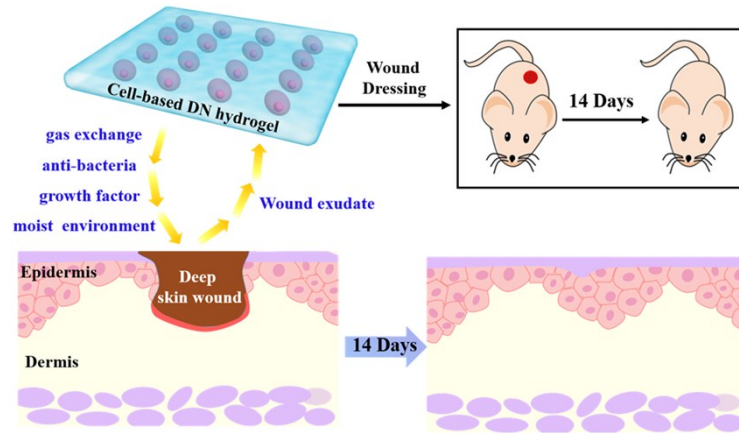


Figure S11. Schematic illustration of cell-loaded D-hydrogel used as wound dressings which provide a suitable environment for wound healing in vivo experiment.